Proceedings of IMECE04
2004 ASME International Mechanical Engineering Congress and Exposition
November 13-20, 2004, Anaheim, California USA

IMECE2004-59562

AN UNSTRUCTURED DISCONTINUOUS FINITE ELEMENT METHOD FOR THREE-DIMENSIONAL RADIATIVE TRANSFER IN PARTICIPATING MEDIA

X. Cui and B. Q. Li
School of Mechanical and Materials Engineering
Washington State University
Pullman, WA 99164

ABSTRACT

This paper presents a discontinuous finite element (or discontinuous Galerkin) computational methodology for the numerical solution of internal thermal radiation problems in three-dimensional geometries using unstructured meshes. Mathematical formulation and numerical details using the discontinuous Galerkin method for internal radiation heat transfer calculations are given. Computational procedures are presented. Numerical examples are given for radiative transfer in 3-D geometries filled with a non-scattering or scattering medium. The computed results are given and are compared well with analytical solutions whenever available or the data reported in references.

Keywords:
Radiation, radiative, absorbing, emitting, scattering, medium, unstructured, discontinuous finite element, DFE, Galerkin.

INTRODUCTION

Radiative transfer is important in many high temperature process applications such as utility boilers, melting furnaces and gas turbulent combustors. Because of its importance, radiative heat transfer involving participating media has been a subject of study for many years and numerous numerical techniques have been developed to obtain computational representations of the radiative intensity distribution in a variety of geometries encountered in engineering applications. The widely used numerical techniques for the solution of radiative transfer equations include the discrete ordinates, finite volume, ray tracing, and Monte Carlo methods [1].

Recently, the discontinuous finite element method, which was first introduced by Reed and Hill [2], has emerged as a viable alternative for the solution of thermal engineering problems. The discontinuous finite element (DFE hereafter) method combines the salient features of both finite volume and finite element methods and has several important advantages over the numerical methods currently in use today, including the finite volume and finite element methods, for the thermal radiation problems. The DFE method is a local method with a higher order accuracy and geometric flexibility. It is particularly useful for the solution of radiative transfer problems involving participating media [3]. It is fairly straightforward and easy to implement within a parallel computing framework, because of its localized nature of formulation. This last feature can be very useful for the computation of thermal radiation problems in three-dimensional calculations, as these types of computations can be very time consuming, especially when scattering media are considered.

In this paper, a discontinuous finite element computational methodology is presented for the solution of three-dimensional thermal radiation problems that involve absorbing, emitting and scattering media. Mathematical formulations and essential numerical details are given for 3-D linear elements. Examples of various degrees of difficulty are given and are compared with available solutions reported in literatures obtained using other numerical methods. The computations used unstructured mesh, which is particularly useful for discontinuous finite element formulations

NOMENCLATURE

I	intensity
L	characteristic length of geometry
n	outward normal of boundary or wall
NB	neighboring element
Nd	number of boundaries of element
N_Ω	total number of control angles
q	heat flux
r	position vector
s,s′	direction vector radiation
S	source function
t	vector
V	volume
Greek	
β	extinction coefficient

ε	emissivity
ϕ	shape function
Φ	scattering phase function
Γ	boundary
φ	polar angle
κ	absorption coefficient
θ	azimuthal angle
σ	Stefan-Boltzmann constant
σ_s	scattering coefficient
ω	scattering albedo
Ω, Ω'	control angles
ΔΩ	solid angle

Subscripts and superscripts

b	black body
e	element
l	the *l*th direction of radiation
*	symmetric vector

2. RADIATIVE HEAT TRANSFER

The radiative transport equation describes the distribution of the radiant intensity $I(\mathbf{r},\mathbf{s})$, which is a function of both coordinates **r** and direction **s**. The governing equation is derived based on the local balance of radiation energy, as shown in Figure 1. For a steady state, which is often the case for radiative heat transfer applications, the transient effects may be neglected and we have the well familiar integral-differential equation for the distribution of radiation intensity [1],

$$\frac{\partial I(\mathbf{r},\mathbf{s})}{\partial s} = -\beta(\mathbf{r})I(\mathbf{r},\mathbf{s}) + \kappa(\mathbf{r})I_b(\mathbf{r}) + \frac{\sigma_s(\mathbf{r})}{4\pi}\int_{4\pi} I(\mathbf{r},\mathbf{s}')\Phi(\mathbf{s},\mathbf{s}')d\Omega' \tag{1}$$

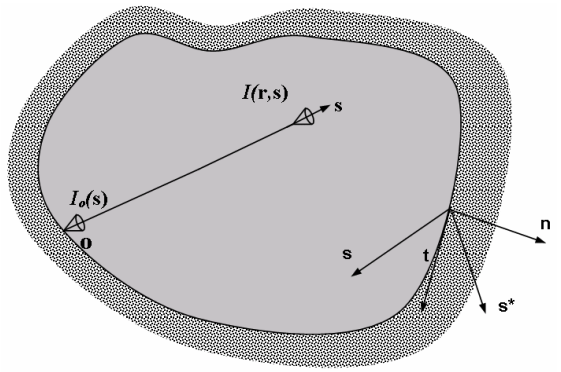

Figure 1

where $\beta(\mathbf{r})=\kappa(\mathbf{r})+\sigma_s(\mathbf{r})$ is the extinction coefficient, $\kappa(\mathbf{r})$ is the absorption coefficient, $\sigma_s(\mathbf{r})$ is the scattering coefficient, and $\Omega(\mathbf{s})$ is the control angle associated direction **s** (**s**= sinθcosφ $\hat{i}$ + sinθsinφ $\hat{j}$ +cosθ $\hat{k}$), with $d\Omega=\sin\theta\, d\theta\, d\varphi$ being the differential solid angle. The phase function satisfies the following condition,

$$\frac{1}{4\pi}\int_{4\pi}\Phi(\mathbf{s},\mathbf{s}')d\Omega' = 1 \tag{2}$$

where **s′** denotes the incident intensity from other directions. The equation is solved subject to the boundary condition on $I(\mathbf{r},\mathbf{s})$, which for an opaque diffuse surface takes the following form,

$$I(\mathbf{r},\mathbf{s}) = \varepsilon(\mathbf{r})I_b(\mathbf{r}) + \frac{1-\varepsilon(\mathbf{r})}{\pi}\int_{\mathbf{s}'\cdot\mathbf{n}>0} I(\mathbf{r},\mathbf{s}')\,\mathbf{s}'\cdot\mathbf{n}\,d\Omega' \tag{3}$$

Symmetry boundary conditions are also used in the computations and are given below [4]

$$\begin{cases} I(\mathbf{r},\mathbf{s}) = I(\mathbf{r},\mathbf{s}^*) \\ \mathbf{n}\cdot\mathbf{s} = -\mathbf{n}\cdot\mathbf{s}^* \\ \mathbf{s}\times\mathbf{s}^*\cdot\mathbf{n} = 0 \end{cases} \tag{4}$$

where the $\mathbf{s}^*$ is the symmetric radiation direction of **s** respect to the tangent of the boundary, with both **s** and $\mathbf{s}^*$ lying on the plane of **t**-**n** (see Figure 1).

Once the distribution of radiation intensity is known, various quantities of interest to internal radiation heat transfer can be calculated. Two of the most important quantities are the heat fluxes and their derivatives [1], which are determined by Eqs. (5) and (6),

$$q(\mathbf{r})\cdot\mathbf{n} = \int_{4\pi} I(\mathbf{r},\mathbf{s})\mathbf{s}\cdot\mathbf{n}\,d\Omega \tag{5}$$

$$\nabla\cdot q(\mathbf{r}) = \kappa(4\sigma T^4(\mathbf{r}) - \int_{4\pi} I(\mathbf{r},\mathbf{s})d\Omega) \tag{6}$$

3. THE DISCONTINUOUS FINITE ELEMENT FORMULATION

We consider the discontinuous finite element formulation for radiative heat transfer problems governed by Eq. (1). As with other methods, the domain first is discretized into a collection of finite elements. In this study, unstructured meshes are used, although tetrahedral elements are always used for 3-D problems below, cubic elements, hexahedral elements or mixed elements also can be used. Here tetrahedral elements are considered, Specifically, we consider the ith element in a 3-D mesh, as shown in Figure 2(a), and integrate Eq. (1) over the element with respect to a weighting function $v(\mathbf{r}, \Omega)$,

$$\int_{\Delta\Omega_l}\int_{V_e} v(\mathbf{r},\Omega)\mathbf{s}\cdot\nabla I dV d\Omega = \int_{\Delta\Omega_l}\int_{V_e} v(\mathbf{r},\Omega)\big(-\beta(\mathbf{r})I(\mathbf{r},\mathbf{s}) + S(\mathbf{r},\mathbf{s})\big)dV d\Omega \tag{7}$$

where V_e is the volume of the element under consideration (i.e. the ith element), **r** = x $\hat{i}$ +y $\hat{j}$ +z $\hat{k}$ and S(**r**, **s**) is the source function defined by

$$S(\mathbf{r},\mathbf{s}) = \kappa(\mathbf{r})I_b(\mathbf{r}) + \frac{\sigma_s(\mathbf{r})}{4\pi}\int_{4\pi} I(\mathbf{r},\mathbf{s}')\Phi(\mathbf{s},\mathbf{s}')d\Omega' \tag{8}$$

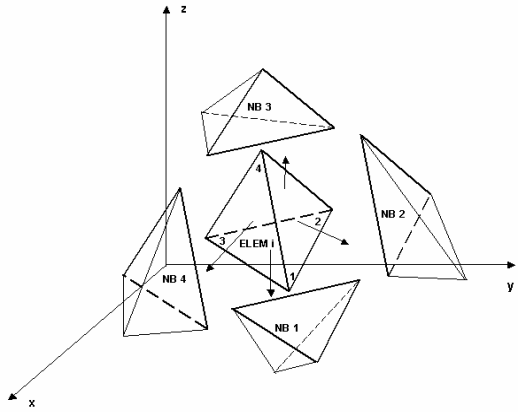

Figure 2(a)

Integration of the above equation once gives

$$\begin{aligned} &-\int_{\Delta\Omega_l}\int_{V_e} I\,\mathbf{s}\cdot\nabla v(\mathbf{r},\Omega)dVd\Omega + \int_{\Delta\Omega_l}\int_{\Gamma} v(\mathbf{r},\Omega)\,I^{+}\,\mathbf{n}\cdot\mathbf{s}\;d\Gamma d\Omega \\ &= \int_{\Delta\Omega_l}\int_{V_e} v(\mathbf{r},\Omega)\big(-\beta(\mathbf{r})I(\mathbf{r},\mathbf{s}) + S(\mathbf{r},\mathbf{s})\big)dVd\Omega \end{aligned} \tag{9}$$

Application of integration-by-parts once again to Eq. (9) yields the following expression,

$$\begin{aligned} &\int_{\Delta\Omega_l}\int_{V_e} v(\mathbf{r},\Omega)\,\mathbf{s}\cdot\nabla I dVd\Omega + \int_{\Delta\Omega_l}\int_{\Gamma} v(\mathbf{r},\Omega)\,[I]\,\mathbf{n}\cdot\mathbf{s}\,d\Omega\,d\Gamma \\ &= \int_{\Delta\Omega_l}\int_{V_e} v(\mathbf{r},\Omega)\big(-\beta(\mathbf{r})I(\mathbf{r},\mathbf{s}) + S(\mathbf{r},\mathbf{s})\big)dV\,d\Omega \end{aligned} \tag{10}$$

where **n** is the outward normal of the element boundary. In the above two equations, use has been made of the divergence theorem,

$$\mathbf{s}\cdot\int_A \phi I\mathbf{n}dA - \mathbf{s}\cdot\int_V I\nabla\phi dV = \mathbf{s}\cdot\int_V \phi\nabla I dV \tag{11}$$

to convert the domain integral into the boundary integral. In Eq. (10), Γ is the boundary enclosing the volume V. Note that **s** is the unit vector of the direction of radiation intensity $I(\mathbf{r},\mathbf{s})$ and is independent of the volume. In the conventional finite element formulation, the terms on the boundary disappear when they are combined with neighboring elements or $[I]$ = 0. In the discontinuous formulation, however, these terms do not cancel when elements are assembled. Instead, the following limiting values are used,

$$I_j^{+} = \lim_{\mathbf{r}_j\to\Gamma^{+}} I(\mathbf{r}_j) \quad \text{and} \quad I_j^{-} = \lim_{\mathbf{r}_j\to\Gamma^{-}} I(\mathbf{r}_j) \tag{12}$$

where the subscripts + refer to being the values outside the element and those by – are inside the element. This definition is slightly different from the one-D case [3] but the essential idea is the same. The treatment of the above assumes that the two values I_j^{+} and I_j^{-} across the element boundaries are not the same, and these jumps are often denoted by,

$$[I]_j = I_j^{+} - I_j^{-} \tag{13}$$

These jumps may also be modeled by the generic numerical fluxes that are single-valued at the boundaries and are a function of field values across the inter-element boundaries [3]. For the problems under consideration, the simplest and yet effective choice is the upwinding, which in the discontinuous finite element literature is some times referred to as the inflow boundary value,

$$[I]_j = \begin{cases} [I]_j & if \quad \mathbf{n}\cdot\mathbf{s} < 0 \\ 0 & if \quad \mathbf{n}\cdot\mathbf{s} > 0 \end{cases} \tag{14}$$

We may now use the appropriate interpolation functions, which may be chosen from the finite element broken space that does not demand continuity across the inter-element boundaries [5]. A natural choice of shape functions for the internal radiation applications is to take a step function for the solid angle and a polynomial function for spatial variation, $v(\Omega,\mathbf{r})=\psi(\Delta\Omega_l)\phi(\mathbf{r})$. Here $\psi(\Delta\Omega_l)$ is the step function of the solid angle differential centered at Ω_l and $\phi(\mathbf{r})$ the shape function of spatial coordinates. Substituting this testing function into the integral expression and re-arranging, one has the following relation,

$$\begin{aligned} &\int_{\Delta\Omega_l}\mathbf{s}\cdot\int_{V_e}\phi\nabla I(\mathbf{r},\mathbf{s})dVd\Omega + \int_{\Delta\Omega_l}\int_{\Gamma}\phi[I](\mathbf{n}\cdot\mathbf{s})d\Gamma d\Omega \\ &= \int_{\Delta\Omega_l}\int_{V_e}[-\beta(\mathbf{r})\phi I(\mathbf{r},\mathbf{s}) + \phi S(\mathbf{r},\mathbf{s})]dVd\Omega \end{aligned} \tag{15}$$

which is the final form of integral presentation of the radiative transfer equation.

Before the numerical implementation is considered, a few points are worthy noting. First, if the jump condition $[I]$ is set to zero in Eq.(15), which means that the inter-element continuity is enforced, then the conventional finite element formulation is recovered. Second, if the zeroth order polynomial is chosen as the spatial interpolation function, then we have the common finite volume formulation. Thus, in this sense, the finite volume method is a subclass of the discontinuous finite element method, and uses the lowest order approximation to the field variables.

4. NUMERICAL IMPLEMENTATION

Let us consider again the ith element and its neighbors as shown in Figure 2(a). For the sake of discussion, the inter-element boundaries are plotted separately. The nodal values of the variable are defined within the element. Since the discontinuity is allowed across the element boundaries, the common geometric node does not have the same field variable value. This is an essential difference between the conventional and the discontinuous finite element formulations.

For a 3-D linear tetrahedral element, the shape functions may be written in terms of natural coordinates,

$$\begin{bmatrix}\phi_1\\ \phi_2\\ \phi_3\\ \phi_4\end{bmatrix}=\begin{bmatrix}\lambda_1\\ \lambda_2\\ \lambda_3\\ \lambda_4\end{bmatrix} \tag{16}$$

Here λ_j (j=1,2,3,4) is defined by the area ratio,

$$\lambda_j=\frac{V_j}{V_e} \tag{17}$$

where V_e is the volume of the element and V_j the volume of sub-tetrahedron formed from point p inside the element and other three vertices except node j (see Figure 2(b)). The shape function for a tetrahedral element has the following form when written in the global coordinate system,

$$\begin{bmatrix}\phi_1\\ \phi_2\\ \phi_3\\ \phi_4\end{bmatrix}=\frac{1}{6V_e}\begin{bmatrix}V_{234} & -X_{234} & -Y_{234} & -Z_{234}\\ -V_{341} & X_{341} & Y_{341} & Z_{341}\\ V_{412} & -X_{412} & -Y_{412} & -Z_{412}\\ -V_{123} & X_{123} & Y_{123} & Z_{123}\end{bmatrix}\begin{bmatrix}1\\ x\\ y\\ z\end{bmatrix} \tag{18}$$

where the definition of elements in Eq(18) are given by,

$$V_{ijk}=\begin{vmatrix}x_i & x_j & x_k\\ y_i & y_j & y_k\\ z_i & z_j & z_k\end{vmatrix},\quad X_{ijk}=\begin{vmatrix}1 & 1 & 1\\ y_i & y_j & y_k\\ z_i & z_j & z_k\end{vmatrix}$$

$$Y_{ijk}=\begin{vmatrix}1 & 1 & 1\\ z_i & z_j & z_k\\ x_i & x_j & x_k\end{vmatrix},\quad Z_{ijk}=\begin{vmatrix}1 & 1 & 1\\ x_i & x_j & x_k\\ y_i & y_j & y_k\end{vmatrix} \tag{19}$$

Here the lower case x_j, y_j and z_j denote the coordinates x, y, and z of jth node of the tetrahedron under consideration (see Figure 2(b)).

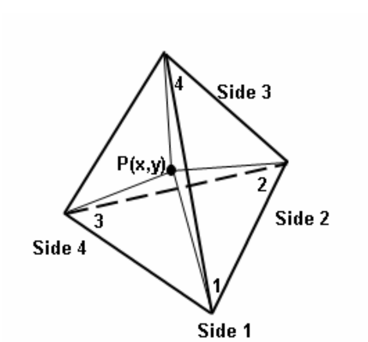

Figure 2(b)

The radiation intensity within a tetrahedron is interpolated by,

$$I(x,y,z;\mathbf{s})=\sum_{i=1}^{4}\phi_i\, I_i(\mathbf{s}) \tag{20}$$
$$=\phi_1 I_1(\mathbf{s})+\phi_2 I_2(\mathbf{s})+\phi_3 I_3(\mathbf{s})+\phi_4 I_4(\mathbf{s})$$

Substituting the above expression into the general formulation Eq. (15), we have

$$\int_{\Delta\Omega_l}\mathbf{s}d\Omega\cdot\int_{V_e}\begin{bmatrix}\phi_1\\ \phi_2\\ \phi_3\\ \phi_4\end{bmatrix}[\nabla\phi_1,\nabla\phi_2,\nabla\phi_3,\nabla\phi_4]\begin{bmatrix}I_1\\ I_2\\ I_3\\ I_4\end{bmatrix}dV$$

$$+\sum_{i=1}^{4}\int_{\Delta\Omega_l}(-\mathbf{n}_i\cdot\mathbf{s})d\Omega\int_{\Gamma}\begin{bmatrix}\phi_1\\ \phi_2\\ \phi_3\\ \phi_4\end{bmatrix}[\phi_1,\phi_2,\phi_3,\phi_4]\begin{bmatrix}[I]_1\\ [I]_2\\ [I]_3\\ [I]_4\end{bmatrix}d\Gamma \tag{21}$$

$$=\int_{\Delta\Omega_l}d\Omega\int_{V_e}\{-\beta(\mathbf{r})\begin{bmatrix}\phi_1\\ \phi_2\\ \phi_3\\ \phi_4\end{bmatrix}[\phi_1,\phi_2,\phi_3,\phi_4]\begin{bmatrix}I_1\\ I_2\\ I_3\\ I_4\end{bmatrix}+\begin{bmatrix}\phi_1\\ \phi_2\\ \phi_3\\ \phi_4\end{bmatrix}S(\mathbf{r},\mathbf{s})\}dV$$

Once again, the derivative of the shape functions can be obtained analytically with the following result,

$$\begin{bmatrix}\nabla\phi_1\\ \nabla\phi_2\\ \nabla\phi_3\\ \nabla\phi_4\end{bmatrix}=\frac{1}{J}\begin{bmatrix}-X_{234} & -Y_{234} & -Z_{234}\\ X_{341} & Y_{341} & Z_{341}\\ -X_{412} & -Y_{412} & -Z_{412}\\ X_{123} & Y_{123} & Z_{123}\end{bmatrix}\begin{bmatrix}\hat{i}\\ \hat{j}\\ \hat{k}\end{bmatrix} \tag{22}$$

where $J=6V_e$ is the Jacobin of tetrahedral element.

This will allow us to analytically integrate the volume terms in Eq. (16) as following equation for the 3-D tetrahedral elements,

$$\int_{\Delta\Omega_l}\int_{V_e}\begin{bmatrix}\phi_1\\ \phi_2\\ \phi_3\\ \phi_4\end{bmatrix}[\mathbf{s}\cdot\nabla\phi_1,\mathbf{s}\cdot\nabla\phi_2,\mathbf{s}\cdot\nabla\phi_3,\mathbf{s}\cdot\nabla\phi_4]dVd\Omega$$

$$=\int_{V_e}\begin{bmatrix}\phi_1\\ \phi_2\\ \phi_3\\ \phi_4\end{bmatrix}dV\int_{\Delta\Omega_l}[\mathbf{s}\cdot\nabla\phi_1,\mathbf{s}\cdot\nabla\phi_2,\mathbf{s}\cdot\nabla\phi_3,\mathbf{s}\cdot\nabla\phi_4]d\Omega$$

$$=\frac{V_e}{4}\begin{bmatrix}\bar{\mathbf{s}}\cdot\nabla\phi_1 & \bar{\mathbf{s}}\cdot\nabla\phi_2 & \bar{\mathbf{s}}\cdot\nabla\phi_3 & \bar{\mathbf{s}}\cdot\nabla\phi_4\\ \bar{\mathbf{s}}\cdot\nabla\phi_1 & \bar{\mathbf{s}}\cdot\nabla\phi_2 & \bar{\mathbf{s}}\cdot\nabla\phi_3 & \bar{\mathbf{s}}\cdot\nabla\phi_4\\ \bar{\mathbf{s}}\cdot\nabla\phi_1 & \bar{\mathbf{s}}\cdot\nabla\phi_2 & \bar{\mathbf{s}}\cdot\nabla\phi_3 & \bar{\mathbf{s}}\cdot\nabla\phi_4\\ \bar{\mathbf{s}}\cdot\nabla\phi_1 & \bar{\mathbf{s}}\cdot\nabla\phi_2 & \bar{\mathbf{s}}\cdot\nabla\phi_3 & \bar{\mathbf{s}}\cdot\nabla\phi_4\end{bmatrix} \tag{23}$$

where $\bar{\mathbf{s}}$ is calculated by,

$$\bar{\mathbf{s}}=\int_{\Delta\Omega_l}\mathbf{s}d\Omega=[0.5(\theta_2-\theta_1)-0.25(\sin 2\theta_2-\sin 2\theta_1)]$$
$$\times[(\sin\varphi_2-\sin\varphi_1)\hat{i}-(\cos\varphi_2-\cos\varphi_1)\hat{j}]$$

$$-0.25(\cos 2\theta_2 - \cos 2\theta_1)(\varphi_2 - \varphi_1)\hat{k} \qquad (24)$$

Note that $\nabla\phi_i$ (i = 1,2,3,4) is defined solely by the nodal coordinates of the tetrahedral element and thus can be taken outside the volume integral. From here on $\int_{\Delta\Omega_l}(\mathbf{n}_j\cdot\mathbf{s})d\Omega$ is denoted by $NDS_{ij,}$ with subscript i referring to the ith element and j the jth side of the element. In the DFE treatment, the jump terms have to be selected depending on the sign of $\mathbf{n}_j\cdot\mathbf{s}$. This is different from the conventional finite element formulation in which the across-element continuity is enforced, and the inter-element boundary terms cancel each other. One treatment that works effectively with linear elements is the upwinding scheme. By this scheme, one has

$$\begin{bmatrix}[I]_1\\ [I]_2\\ [I]_3\\ [I]_4\end{bmatrix} NDS_{ij} = \max(0,-NDS_{ij})\left\{\begin{bmatrix}I_1\\ I_2\\ I_3\\ I_4\end{bmatrix}_{Elem\,i} - \begin{bmatrix}I_1\\ I_2\\ I_3\\ I_4\end{bmatrix}_{NBj}\right\} \qquad (25)$$

where $I_{k,NBj}$ denotes the node k of neighbor element which shares the boundary j of the element i. By the same token, the calculations for other two sides can also be performed analytically. Note that $(I_j)_{NB} = (I_j{}^+)_{Elem\,i}$ by definition (see Figure 2). The results are summarized below for convenience,

$$\int_{\Gamma_j}\begin{bmatrix}\phi_1\\ \phi_2\\ \phi_3\\ \phi_4\end{bmatrix}[\phi_1,\phi_2,\phi_3,\phi_4]\begin{bmatrix}[I]_1\\ [I]_2\\ [I]_3\\ [I]_4\end{bmatrix}d\Gamma\int_{\Delta\Omega_l}(\mathbf{n}_j\cdot\mathbf{s})d\Omega$$

$$= \frac{A_j}{12}CofC_{(5-j,5-j)}\max(0,-NDS_{ij})\left\{\begin{bmatrix}I_1\\ I_2\\ I_3\\ I_4\end{bmatrix}_{Elem\,i} - \begin{bmatrix}I_1\\ I_2\\ I_3\\ I_4\end{bmatrix}_{NBj}\right\} \qquad (26)$$

where Cof C_{kl} is the matrix by setting to zero the elements in the *k*th row and the *l*th column of the matrix C, which is defined by

$$C = \begin{bmatrix}2&1&1&1\\ 1&2&1&1\\ 1&1&2&1\\ 1&1&1&2\end{bmatrix} \qquad (27)$$

Assembling all these discretized terms together, the equation for the element can be written in terms of the following matrix form,

$$[K]\{I\} = \{f\} \qquad (28)$$

where the expressions for the matrix elements are summarized as follows,

$$k_{ij} = \int_{V_e}\phi_i\nabla\phi_j dV\cdot\int_{\Delta\Omega_l}\mathbf{s}\,d\Omega + \beta\int_{\Delta V}\phi_i\phi_j dV\int_{\Delta\Omega_l}d\Omega + \sum_{k=1}^{Nd}\max(0,-\int_{\Delta\Omega_l}\mathbf{s}\cdot\mathbf{n}_k d\Omega)\int_{\Gamma_k}\phi_i\phi_j d\Gamma \qquad (29)$$

$$f_i = \int_{V_e}\phi_i S dV\int_{\Delta\Omega_l}d\Omega + \sum_{k=1}^{Nd}\max(0,-\int_{\Delta\Omega_l}\mathbf{s}\cdot\mathbf{n}_k d\Omega)\int_{\Gamma_k}\phi_i\phi_j I_{NB}d\Gamma \qquad (30)$$

with Nd being the number of boundaries associated with the ith element.

The boundary condition is imposed for a gray boundary as follows,

$$I^+(\mathbf{r},\mathbf{s}_l) = \varepsilon(\mathbf{r})I_b(\mathbf{r})$$

$$+\frac{1-\varepsilon(\mathbf{r})}{\pi}\sum_{j=0,\mathbf{s}_j'\cdot\mathbf{n}>0}^{N_\Omega}I^-(\mathbf{r},\mathbf{s}_j')\left|\mathbf{s}_j'\cdot\mathbf{n}\right|\Delta\Omega'_j \qquad (31)$$

and the following equation is for the symmetry boundary condition,

$$I^+(\mathbf{r},\mathbf{s}_l) = I^-(\mathbf{r},\mathbf{s}_l^*) \qquad (32)$$

Here $\mathbf{s}^*$ is the symmetric direction of $\mathbf{s}$ respected to the boundary, and can be calculated by Eq (4). Note that Eq (28) can be obtained for each element and its neighbors and the calculations are then performed element by element. Thus, with Eq. (28), the calculation for the ith element starts with selecting a direction and continues element by element until the entire domain and all directions are covered. Because of the boundary conditions, iterative procedures are required. The successive substitution method seems to work well for this type of problems. Here another important quantity of radiation is the incidence of radiation, which is defined as

$$G(r) = \int_{4\pi}I(\mathbf{r},\mathbf{s})d\Omega = \sum_{i=1}^{N_\Omega}I(\mathbf{r},\mathbf{s})\Delta\Omega_i \qquad (33)$$

The convergence criterion can be represented by incidence of radiation as

$$\max\left(\left|\frac{G^{n+1}(r)-G^n(r)}{G^n(r)}\right|\right)\le 1.0\times10^{-4} \qquad (34)$$

where, n is the iteration number. After all elements are calculated, the intensity at a node is averaged within the elements around this node, and then to test if the convergence criterion is reached. After convergence, radiative heat flux and the divergence of radiative heat flux is obtained by Eqs. (5) and (6).

In the above, it is assumed that the medium is not scattering and thus the scattering term is set to zero. When the scattering term is known, it can be readily calculated using the Gaussian integration and included in the force vector $\{f\}$.

5. RESULTS AND DISCUSSION

In this section, the discontinuous finite element algorithm is applied to solve the problems of thermal radiation heat transfer in participating media. The calculations may use either structured or unstructured meshes, though the results computed with the latter are presented below. The gray participating media are used for all the cases considered here, unless otherwise indicated, all the data are nondimensionalized.

Case 1. Radiation in 3-D geometry

Here, a cube enclosure is filled with an emitting and absorbing medium, but no scattering. The length of cube is L=1 and cube is discretized into 2,313 unstructured tetrahedral elements, as shown in figure 3(a). Again, the unstructured 3-D mesh is generated using the front advancing technique [6]. The control angles used in this problem is 4x8, that is, the angular space is divided into 4 in the azimuthal direction (θ) and 8 in the polar direction (φ), which is shown in Figure 2(c).

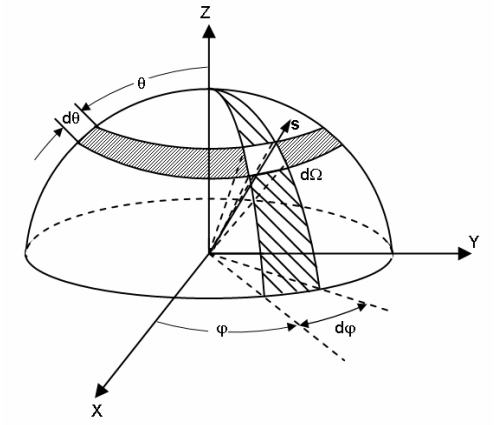

Figure 2(c)

The temperature of the medium is set at T_{ref}=constant. In order to check the accuracy of the DFE method in 3-D calculation, the following boundary conditions are specified in this problem so that analytical solution can be obtained for comparison. For this purpose, the top (z = 1) and bottom (z = 0) surfaces are set as black and cold walls, which denote the temperature of wall is zero and emissivity of wall ε=1.0, but all four lateral surfaces are applied with symmetry boundary condition.

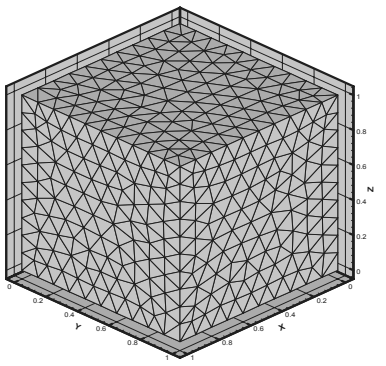

Figure 3(a)

The analytical solution is derived by integrating the RTE equation, and has the following expression as given by Eq. (35) [1],

$$q(z) = 2\pi\int_0^z I_b(z')E_2(z-z')dz' - 2\pi\int_z^1 I_b(z')E_2(z'-z)\,dz' \qquad (35)$$

where I_b is the black body radiation intensity and $E_n(x)$ is the exponential integral function [1],

$$E_n(z) = \int_0^1 \mu^{n-2}\exp\left(\frac{-z}{\mu}\right)d\mu \qquad (36)$$

Figure 3(b) shows the calculated heat fluxes q_z^* along z/L at center line of cube where x/L=0.5, and y/L=0.5. The extinction coefficient is β=0.1, β=0.5, β=1.0, and β=10 respectively. From the figure, it is clear that the DFE method gives good results compared with analytical solutions for a wide range of β values, and for convenience the radiative heat flux in this paper is nondimensionalized as Eq. (37).

$$q^* = \frac{q_r}{\sigma T_{ref}^4} \qquad (37)$$

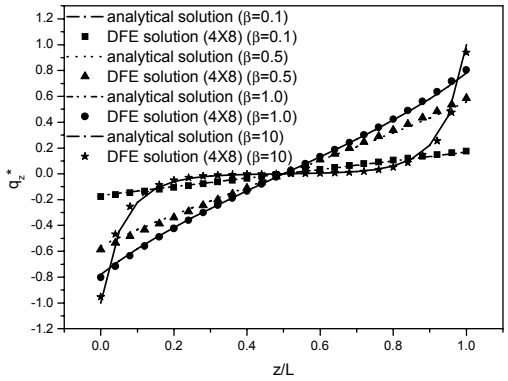

Figure 3(b)

Case 2. Radiation in irregular 3-D geometry

In this case, a 3-D tetrahedral enclosure formed by the vertices (0, 0, 0), (1, 0, 0), (0.5, 0.866, 0.0) and (0.5, 0.218, 0.817) is chosen, and the enclosure is filled with an emitting and absorbing medium. The temperature of the medium is constant T_{ref}, and the absorption coefficient κ=1.0. Meanwhile temperature of all boundary walls is 0 and emissivity is 1.0. The domain is discretized into 1062 unstructured tetrahedral (see Figure 4(a)).

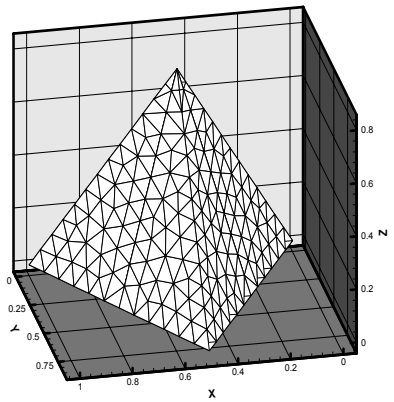

Figure 4(a)

The heat fluxes q* along the line joining the point (0.75, 0.433, 0) and (0.5, 0.218, 0.817) is calculated by DFE method as shown in Figure 4(b), where q* denotes the nondimensionalized boundary heat flux in outward normal direction of the boundary. The result is compared well with Ray tracing method, which is reported by Murthy and Mathur [7].

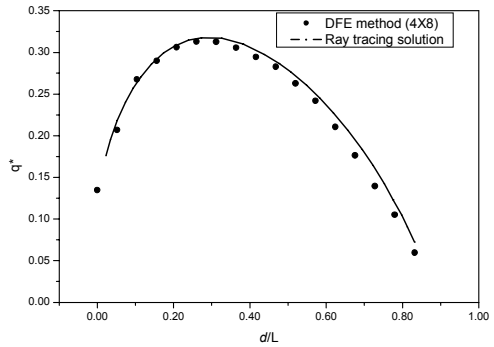

Figure 4(b)

Case 3. Scattering in 3-D geometry

When fine particles are present in the medium, they scatter the radiation of a given direction into all other directions. Radiation in other directions may also be scattered into the direction under consideration in a scattering medium. Scattering effect is included as part of the source term for radiation transfer (i.e. the second term on the right hand side of Eq. (8)). Scattering effects are usually classified into two categories, isotropic scattering and anisotropic scattering. The former scatters energy to all other directions with the same energy distribution, whereas the latter scatters radiation energy to different directions with varying energy distributions. The isotropic scattering function is simple and is calculated by Eq. (38),

$$\Phi(\mathbf{s},\mathbf{s}') = 1 \tag{38}$$

Anisotropic scattering is more complex and certainly needs more computing time since the scattering function is directionally dependent, and all directions need to be calculated. In general, there are two different models being used for anisotropic scattering functions [8], this is, forward scattering and backward scattering. The forward scattering means more energy is scattered into the forward directions than the backward directions. The backward scattering means just opposite, that is, more energy is scattered into backward direction. The scattering functions, either forward or backward, may be described by the following generic expression,

$$\Phi(\mathbf{s},\mathbf{s}') = \sum_{j=1}^{Ns} c_j P_j(\cos\varpi) \tag{39}$$

where N_s is the number of terms of the series and ϖ is calculated by

$$\varpi = \cos\theta\cos\theta' + (1-\cos^2\theta)(1-\cos^2\theta')^{1/2}\cos(\varphi'-\varphi) \tag{40}$$

and P_j is the Legend's polynomial, which can be calculated by Eq (41)

$$\begin{cases} p_0(x) = 1 \\ p_1(x) = x \\ p_{n+1}(x) = \dfrac{2n+1}{n+1}xp_n(x) - \dfrac{n}{n+1}p_{n-1}(x) \end{cases} \tag{41}$$

For the calculations given here, the values of coefficient C_j in Eq(39) are taken from Kim and Lee's work [8], who gave the coefficients of the polynomial for different models by slightly modifying Mie coefficients [9], Özisik's [10] and Siegel's work [1]. Based on these coefficients, the four different scattering functions are depicted in Figure 5(a), where F_i (i=1,2) denotes the forward scattering functions and B_i (i=1,2) the backward scattering functions.

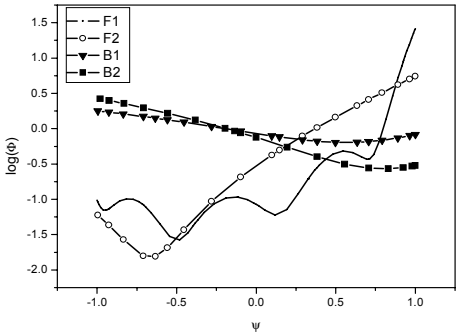

Figure 5(a)

Eqs. (39) and (40) describe the dependence of the scattering function on the directions for anisotropic scattering phenomena. In calculations, the angular space is discretized into finite number of control angles. Often an averaged scattering function over a discretized control angle is used. While the scattering function at the axel direction of control angle may be used as average scattering function, a better approach is to average the scattering function over each control angle using the following expression [11],

$$\overline{\Phi}(\mathbf{s},\mathbf{s}') = \frac{\int_{\Delta\Omega}\int_{\Delta\Omega'} \Phi(\mathbf{s},\mathbf{s}')d\Omega d\Omega'}{\int_{\Delta\Omega}\int_{\Delta\Omega'} d\Omega d\Omega'} \tag{42}$$

The above procedure and scattering functions can be readily incorporated into the discontinuous finite element formulation as a source term, and integrate the term using the integration quadrature rules,

$$\int_{V_e} \frac{\sigma_s(\mathbf{r})}{4\pi} \int_{\Delta\Omega_l} \sum_{j=1}^{N\Omega} \int_{\Delta\Omega'_j} I(\mathbf{r},\mathbf{s}'_j)\Phi(\mathbf{s},\mathbf{s}')d\Omega' d\Omega dV$$
$$= \sum_{k=1}^{N_k} \frac{\sigma_s(\mathbf{r})}{4\pi} W_k \sum_{j=1}^{N\Omega} I(\mathbf{r}_k,\mathbf{s}'_j)\overline{\Phi}(\mathbf{s}_l,\mathbf{s}'_j)\Delta\Omega_l\Delta\Omega'_j \tag{43}$$

where N_k is the number integration points and W_k is the weight of the kth integration point. N_Ω is the number of control angles.

In this case, we use the same problem with case1, except the absorption coefficient and extinction coefficient are changed. For different scattering phase functions, Figures 5(b) shows the heat flux q* distributions along x/L at the line y/L=0.5 and z/L=1.0 on the top surface of the cube with scattering albedo $\omega=\sigma/\beta=0.5$ and $\beta=1.0\ m^{-1}$, and Figure 5(c) shows the heat flux q* distributions along the same line as Figure 5(b) except scattering albedo $\omega=\sigma/\beta=0.5$ and $\beta=2.0\ m^{-1}$. It is clear that for different phase function, the heat flux distribution we obtained are different.

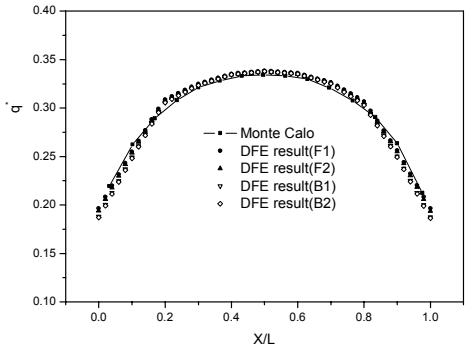

Figure 5(b)

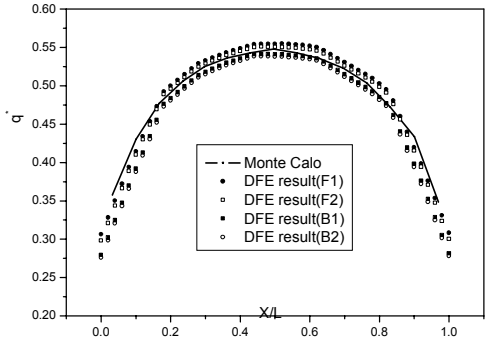

Figure 5(c)

One set of results for isotropic scattering is given in Figure 6. The same unstructured mesh as in Case 3 is used for these computations, with the scattering albedo is $\omega=\sigma/\beta=0.5$ and $\beta=1.0$. The present calculations are also compared with those obtained using the Monte Carlo method and finite volume method. The comparison between the DFE results and those reported [12] is gratifying for all these cases, suggesting that the DFE method is useful for the radiative heat transfer calculations.

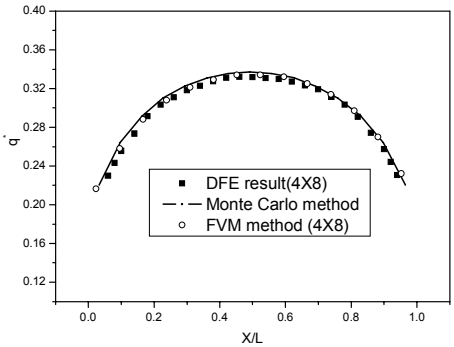

Figure 6

7. CONCULDING REMARKS

This paper has presented a discontinuous finite element formulation for fully three-dimensional radiative heat transfer problems involving absorbing, emitting and scattering media. Mathematical formulations and essential numerical details using the discontinuous Galerkin finite element method for internal radiation heat transfer calculations are given for 3-D tetrahedral linear elements. Extension of these calculations using higher order elements can be readily incorporated through numerical integration. While the computations used unstructured meshes only, they are equally applicable to structured meshes. The computed results obtained by using the discontinuous finite element method are compared well with analytical solutions whenever available or those reported in references. Examples include both non-scattering and scattering cases.

ACKNOWLEDGMENTS

The authors gratefully acknowledge the support of this work by the Air Force Office of Research, subcontracted through VLOC, Inc. (Grant No. VAN00138704451) and by NASA (Grant No: NAG8-1693). The assistance of Dr. Xin Ai with the unstructured mesh generation is also acknowledged.

REFERENCES

1. R. Siegel, and J.R Howell, Thermal Radiation Heat Transfer, 3rd ed., Hemisphere Publishing Company, Washington, D.C., 1992.
2. X. Cui, and B.Q. Li, A Discontinuous Finite Element Formulation for Internal Radiation Problems, Numerical Heat Transfer, B: fundamentals, vol. 46, pp.1-20, 2004.
3. W.H. Reed and T.R. Hill, Triangular Mesh Methods for the Neutron Transport Equation, Technical Report LA-UR-73-479, Los Alamos Scientific Laboratory, 1973.
4. J. P. Moder, G. N. Kumar, and J. C. Chai, An Unstructured-Grid Radiative Heat Transfer Module for the National Combustion Code, 38th Aerospace Sciences Meeting & Exhibit, Reno, NV, 2000.
5. J.T. Oden, I. Babuka, and C. Baumann, A discontinuous hp finite element method for diffusion problems, Journal of Computational Physics, vol.146, n.2, pp.491-519, 1998.
6. S.H. Lo, A New Mesh Generation Scheme for Arbitary Planar Domains, International Journal for Numerical Methods in Engineering, vol.21, pp.1403-1426, 1985.
7. J.Y. Murthy, and S.R. Mathur, Finite Volume Method for Radiative Heat Transfer Using Unstructured Meshes. Journal of Thermophysics and Heat Transfer, vol.12, n.3, pp.313-321, 1998.
8. T.K Kim, and H. Lee, Effect of Anisotropic Scattering on Radiative Heat Transfer in Two-Dimensional Rectangular Enclosures, Journal of Heat Mass Transfer, vol.31, n.8, pp.1711-1721, 1998.
9. W. J. Wiscombe, Improved Mie Scattering Algorithms, *Appl. Optics* vol.19, n.9, pp.1505-1509, 1980.
10. M.N. Özisik, Radiative Transfer, pp.83, Wiley-Interscience, New York, 1973.
11. J.C. Chai and S.V. Patankar, Finite Volume Method For Radiation Heat Transfer, Advances in Numerical Heat Transfer, vol.2, Taylor & Francis, 2000.
12. S.H. Kim and K.Y. Huh, A New Angular Discretization Scheme of the Finite Volume Method for 3-D Radiative Heat Transfer in Absorbing, Emitting and Anisotropically Scattering Medium, International Journal of Heat and Mass Transfer, vol.43, pp.1233-1242, 2000.